Interaction of photons with a coupled atom-cavity system through a bidirectional time-delayed feedback

Hamidreza Chalabi and Edo Waks

Phys. Rev. A **98**, 063832 — Published 21 December 2018

DOI: 10.1103/PhysRevA.98.063832

Interaction of photons with a coupled atom-cavity through two-sided time-delayed feedback

Hamidreza Chalabi* and Edo Waks†
Department of Electrical and Computer Engineering,
The University of Maryland at College Park, College Park, MD 20742, USA

In this work, we have developed a method for describing the dynamics of an arbitrary quantum system under a bidirectional time-delayed feedback loop. For this purpose, we have described the evolution in terms of the time propagation of the quantum system of interest without feedback together with several identical systems which represent the history of the quantum system under study. This technique provides a numerically efficient solution for describing a system's dynamics in the case of significant time delays in which direct investigation of the state of the reservoirs becomes numerically intractable. Using this method, we have studied two scenarios of multiple scatterings of photons incident on a cavity with a two-level atom positioned inside it, coupled to two waveguides that are connected at their ends. In the first scenario, two photons impinge on the cavity through separate waveguides with a delay between them. We have demonstrated that the maximum difference between the two output photon numbers occurs when the delay between the incident photons becomes close to the inverse of their linewidth. In the second scenario, multiple photons impinge on the cavity through the same waveguide and go through multiple interactions. We have shown that for a fixed atom-cavity coupling rate, the transmission rate enhances as the number of photons increases and have quantified this enhancement. The developed method enables us to study a broad range of nonlinear dynamics in complex quantum networks.

INTRODUCTION

Feedback has proven to be of fundamental importance for controlling and stabilizing classical systems [1–6]. Quantum computation and processing also require the design of feedbacks to control and manipulate the dynamics of quantum systems [7–16]. For this purpose, in the past decade, scientists have employed measurement-based feedback for such systems. In this technique the output signal of an open quantum system is measured to tune the system accordingly in real time. More recently, coherent quantum feedback, in which a quantized field scattered by the quantum system is redirected back into the system, has been proposed. This technique can provide faster control relative to the more conventional measurement-based feedback due to its ability to preserve the quantum character of the feedback [17].

In previous studies, scientists have mostly treated coherent quantum feedbacks by assuming that time delays in the connections are negligible. There are techniques [18–22] to describe a quantum network [23–25] made out of different quantum systems connected together when time delays in the connections can be ignored. These techniques also work in the presence of finite time delays for the special case of cascaded systems [26], in which each system drives the subsequent one without the presence of any feedback connection. Nonetheless, time delays are generally unavoidable in practice [27–34]. This is particularly true for optical approaches of implementing coherent quantum feedbacks in large, complex quantum networks. Recently, Grimsmo has developed a theory for time-delayed coherent quantum feedback [35]. In this work, he has studied a general quantum system coupled at two different points to a bosonic reservoir. In this configuration, the out-coupled field from the first point returns back and interacts with the system at the second point, creating a unidirectional feedback [35]. He has demonstrated that the dynamics of such system can be explained by the dynamics of an artificial series of cascaded quantum systems, in which the past versions of the system drive the current version. A separate study [36, 37] has treated unidirectional time-delayed feedback by directly analyzing the state of the reservoir (which represents the feedback connection) as a one dimensional bosonic chain using a matrix product state [38–49]. Nonetheless, the above-mentioned techniques, developed to model unidirectional feedbacks, are unable to describe systems with more complex feedback configurations.

In this work, we have developed a theoretical method to study the dynamics of an arbitrary quantum system driven by a bidirectional feedback loop. In this configuration, the system of interest interacts at two points with a closed bosonic reservoir. Similar to a system under unidirectional feedback, the out-coupled field from the first point returns back and interacts with the system at the second point. However, in contrast to a unidirectional feedback, the out-coupled field from the second point also returns back and interacts with the system at the first point. Thus, this configuration creates two consecutive time-delayed feedbacks. In the developed method, we obtain the evolution of the system under the effect of feedback via the evolution of a quantum cascade of the actual system together with its replicas which represent its past history [26]. We then obtain the system's density

* hchalabi@umd.edu
† edowaks@umd.edu

matrix using a generalized trace operation of the evolution operator in the Hilbert space of the system and its replicas. By viewing the system of interest as a scatterer, one can use this method to study the scattering properties of multiple incident photons. Based on this view, the developed method provides a platform to study the scattering of multiple photons from an arbitrary number of atoms separated from each other which has been the subject of recent investigations [50–58]. Here, we use this method to study two different systems. First, we consider the case of a cavity under a bidirectional feedback made out of two waveguides. In contrast to a cavity under a unidirectional feedback in which the cavity photon number reaches a steady state value, in this case the cavity photon number shows an oscillatory behavior over time. Secondly, we consider an atom-cavity coupled to two waveguides. We study two different scenarios of scatterings from this system which cannot be described using a unidirectional feedback. In the first scenario, two photons impinge on the cavity through separate waveguides with a delay between them. We demonstrate that the maximum deviation of the output photon numbers from one occurs when the delay becomes close to the inverse of the linewidth of photons. In the second scenario, multiple photons impinge on the cavity through the same waveguide and go through multiple interactions. We show that for a fixed atom-cavity coupling rate, the transmission rate increases as the number of photons increases. Our calculations quantify the enhancement of transmission by increasing the number of photons during each round of interaction.

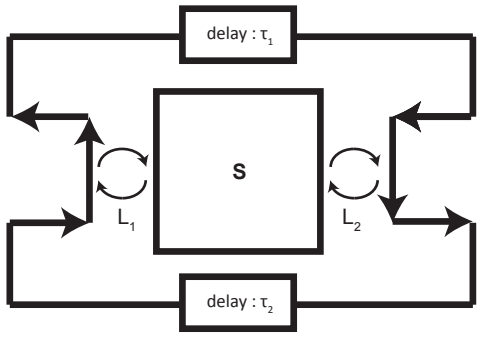

(a)

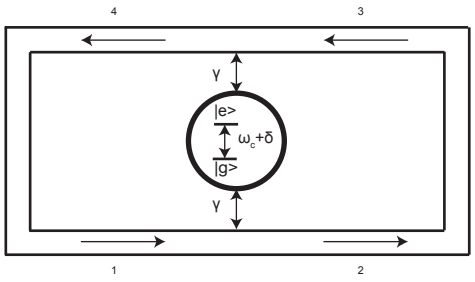

(b)

Figure 1: (a) A system under a bidirectional feedback loop made out of two feedbacks with arbitrary time delays. (b) A system of an atom-cavity that is coupled to two waveguides connected at their ends.

THEORETICAL ANALYSIS

We consider the effect of a bidirectional feedback loop made out of two feedbacks with arbitrary time delays in a general quantum system. As Fig. 1a shows, we have assumed that the output of the system coupled to the delay line will interact with the system after a delay time of τ_1 and the resulting output will interact again with the system after another delay time of τ_2. The delay line in this configuration can in practice be implemented through waveguides. The coupling operators between the delay line and the system are defined as L_1 and L_2. The possible extra phase shift of photons passing through the delay line (caused for instance by the reflection from a mirror) can be absorbed into these coupling operators. Extending the method of system replicas introduced in ref. [35], we have obtained a full description for the evolution of a system under a bidirectional time-delayed feedback loop. The details of the method can be found in the appendix. In the first part of the appendix, the case of feedbacks with similar time delays ($\tau_2 = \tau_1 = \tau$) is considered. The more general case of feedbacks with different time delays ($\tau_2 \neq \tau_1$) is considered in the subsequent part. The use of system replicas to describe the evolution of the system under a time-delayed feedback loop is beneficial for long delays as it does not require storing the reservoir's state [36, 37].

In this method, by defining the base unit of the time delay τ as the common factor of τ_1 and τ_2, in order to obtain the evolution of the system to any time t with $k\tau < t < (k+1)\tau$, k replicas are required as explained in the appendix. Denoting the time propagation of the system and its k replicas between time t_1 and t_2 as $U_k(t_1, t_2)$, the evolution operator for the actual system under the feedback can be expressed in terms of the generalized trace operation of $U_k(t_1, t_2)$ as $U = Tr_{S_{k+1},S_k} \ldots Tr_{S_2,S_1}[U_{k-1}(\tau, s)\, U_k(s, 0)]$. Moreover, all the statistics of the out-coupled photons at the two ports of L_1 and L_2, such as their rates as well as their second correlations, can be expressed with similar generalized trace operations. Note that the case of unidirectional time-delayed feedback, considered in ref. [35], can be treated as a special case of bidirectional feedback considered here by $\tau_1 = \tau$ and $\tau_2 = \infty$.

The time propagation of the system and its k replicas is obtained based on the effective Hamiltonian and the Lindblad operators of the stacked systems. The effective Hamiltonian of the stacked systems is given by $H_{eff} = \sum_{q=0}^{k} H_S^{(q+1)} + V_{int}$, in which the interaction term V_{int} depends on the ratio of τ_2/τ_1. For the special case of $\tau_2 = \tau_1$, the interaction term is given by:

$$V_{int} = \frac{i}{2}\sum_{q=0}^{k-1}\sum_{j=q+1}^{k} L^{(q+1)\dagger}_{q \bmod 2+1} L^{(j+1)}_{j \bmod 2+1} + \frac{i}{2}\sum_{q=0}^{k-1}\sum_{j=q+1}^{k} L^{(q+1)\dagger}_{(q+1) \bmod 2+1} L^{(j+1)}_{(j+1) \bmod 2+1} + h.c.$$

In these equations, $L^{(j)}_{1,2}$ and $H^{(j)}_S$ represent the coupling operators and the Hamiltonian for j^{th} system, respectively. The Lindblad operators of the stacked systems are also dependent on τ_2/τ_1 ratio. For the special case of $\tau_2 = \tau_1$, there exists two Lindblad operators that are given by:

$$L_F = \sum_{q=0}^{k} L^{(q+1)}_{(q+1) \bmod 2+1}$$

$$L_B = \sum_{q=0}^{k} L^{(q+1)}_{q \bmod 2+1}$$

Similar expressions can be obtained for other choices of τ_2/τ_1 ratios. For several of such choices, the corresponding effective Hamiltonian and Lindblad operators have been obtained in the appendix.

This method can be utilized to study multiple scattering events of photons passing through connected waveguides from an arbitrary system that is coupled to them. Note that the waveguides are assumed to be chiral so that the out-coupled photons traverse through them in one-direction [29, 59, 60]. Moreover, the parameters of the system under investigation, such as its Hamiltonian and its coupling operators, can in general be variable with time. For instance, by assuming that one of the coupling operators (e.g., L_1) is zero during the first time delay, and by tuning the other coupling operator (e.g., L_2) as well as the initial Hamiltonian, we have the flexibility to adjust the characteristics of the out-coupled photons, such as their frequency and line-width.

By applying this method to the simple case of a cavity under a bidirectional time-delayed feedback loop, we have studied the evolution of the cavity for several choices of τ_1 and τ_2. These results are summarized in the appendix. In the following sections, however, we have applied the method to study the scattering of photons from a cavity with a single two-level atom positioned inside it during multiple rounds of interactions. In this study, we assume that the atom-cavity interaction Hamiltonian is given by $H_{int} = \hbar g(a^\dagger\sigma_- + a\sigma_-^\dagger)$, in which σ_- is the atomic lowering operator and a is the cavity mode annihilation operator and g is the atom-cavity coupling rate. The schematic of the system under study is shown in Fig. 1b. First, we analyze the effect of delay between two photons moving along separate waveguides impinging on an atom-cavity system. In the subsequent section, we investigate several rounds of interaction of multiple photons impinging on the cavity with an atom inside.

THE EFFECT OF DELAY BETWEEN TWO INCIDENT PHOTONS TO A CAVITY

Using the developed method, in this section we study the scattering of two photons moving along separate waveguides that are connected at their ends from a cavity with a resonant atom inside. In order to initialize the two impinging photons, a feeder cavity in addition to the actual cavity is needed. Assuming that the waveguides provide similar time delays ($\tau_1 = \tau_2 = \tau$), in the first time delay, the photon inside the actual cavity decouples into the bottom waveguide (through path #2 in Fig. 1b) and the photon inside the feeder cavity decouples into the top waveguide (through path #4 in Fig. 1b). Note that the atom-cavity coupling rate is set to zero for the Hamiltonian in this first initialization time delay. In the subsequent time delay, the couplings of the feeder cavity are set to zero while the actual cavity is equally coupled to the two waveguides. In order to provide a delay, Δ, between the out-coupled photons in reaching the interacting cavity, the coupling rate for the feeder cavity can be set to zero for a specific fraction of the first time delay. The interaction between the two photons and the cavity occurs during the second time delay (between τ and 2τ). By integrating the photon rates in the two waveguides during this time delay, we calculate the average number of photons that decouple to the top or bottom waveguides. The results of these calculations are summarized in Fig. 2.

As it can be inferred from this figure, depending on the delay between the impinging photons, the average number of photons that decouple to the top or bottom waveguides varies. It is clear based on the symmetry that for the case of zero delay, these average photon numbers should be equal to one. Moreover, for a zero atom-cavity coupling rate, these average numbers are again equal to one. However, for non-zero delays, increasing the atom-cavity coupling rate will induce a difference between these two average numbers, which will diminish to zero for very large values of atom-cavity coupling rates. Fig. 2a exhibits the results for the case when the two incident photons are generated by decoupling from cavities with similar decay rates as the interacting cavity ($\gamma_{inc} = \gamma$). Fig. 2b depicts the results for the case when the two incident photons are decoupled from cavities with 0.04-times the decay rate of the interacting cavity, resulting in a much narrower line width of the interacting photons ($\gamma_{inc} = 0.04\gamma$). These figures show that the maximum deviation of the output photon numbers from one occurs when $\gamma_{inc}\Delta \sim 1$. Note also that there is a small dip in the average photon numbers in both cases for very small atom-cavity coupling rates, g. This is due to the finite amount of delay time, τ, which will lead to a non-zero excitation of the atom after the delay time for such atom-cavity coupling rates. To minimize these issues, we chose a delay time that is large enough for the preparation of the initial incident photons, such that $\gamma\tau = 1024$ and $\gamma\tau = 128$, respectively, for the cases of $\gamma_{inc} = 0.04\gamma$ and

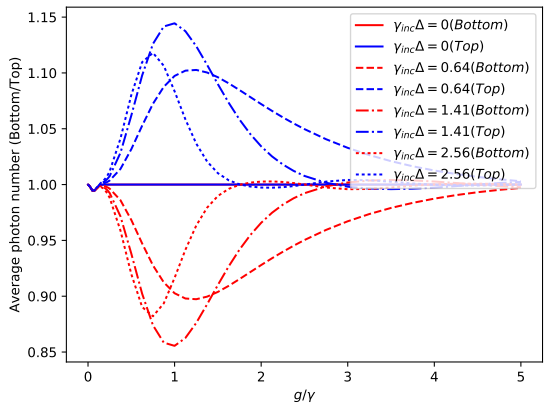

(a)

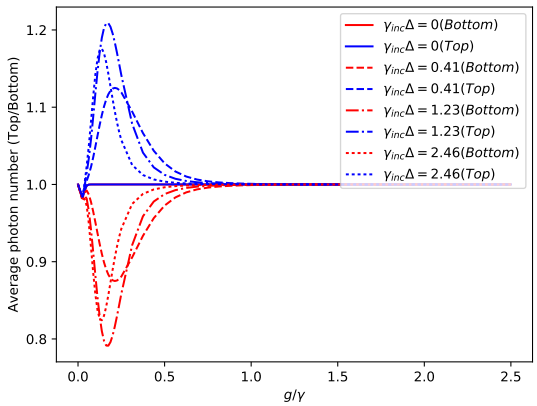

(b)

Figure 2: Average photon numbers decoupled to the top or bottom waveguides as a function of atom-cavity coupling rate for different delays between the incident photons and their decoupled rate of (a) $\gamma_{inc} = \gamma$ and (b) $\gamma_{inc} = 0.04\gamma$.

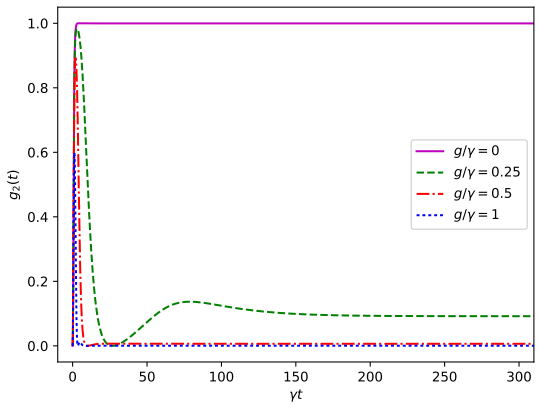

(a)

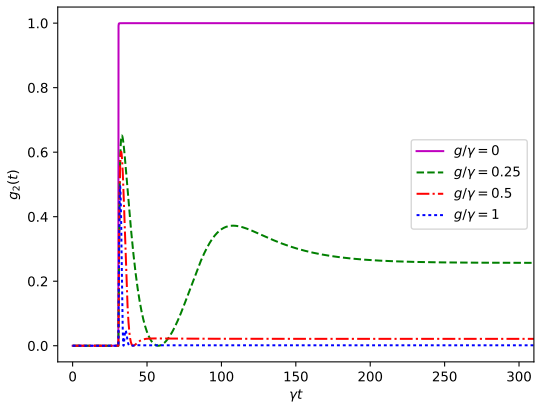

(b)

Figure 3: $g_2(t)$ as a function of time for the photons decoupled to the top waveguide for delays of (a) $\gamma_{inc}\Delta = 0$ and (b) $\gamma_{inc}\Delta = 1.23$.

$\gamma_{inc} = \gamma$.

In addition to the g_1 calculations, we can also obtain other statistics of the output photons. Of special interest is the second order correlation function, which is defined as:

$$g_2(t) = \frac{\left\langle b_{out}^{\dagger}(t)\, b_{out}^{\dagger}(0)\, b_{out}(0)\, b_{out}(t)\right\rangle}{\left\langle b_{out}^{\dagger}(0)\, b_{out}(0)\right\rangle \left\langle b_{out}^{\dagger}(t)\, b_{out}(t)\right\rangle}$$

For the case of $\gamma_{inc} = 0.04\gamma$, which closely models monochromatic photons, the second order correlation function for the decoupled photons in the top waveguide is shown in Figs. 3a and 3b. In these figures, two cases of zero delay, as well as $\gamma_{inc}\Delta = 1.23$, have been considered. As we expect, $g_2(t)$ is zero before the delay time since the other photon has not arrived yet. After this delay time, $g_2(t)$ ramps up and reaches its peak value caused by the stimulated emission. Time variation of $g_2(t)$ is followed by damped oscillations until reaching the steady state value, with a settling time proportional to $2\pi/g$.

INTERACTION OF PHOTONS WITH THE CAVITY DURING MULTIPLE TIME LOOPS

The developed method can also be used for the investigation of the several interactions of multiple photons and a cavity with either atoms inside it or not. The case of a single photon interaction with the cavity with an atom inside it has been studied analytically [61, 62]. In this case, the scattering of a single photon impinging upon a cavity can be described as [61, 62]:

$$\begin{bmatrix} a_{out} \\ b_{out} \end{bmatrix} = \begin{bmatrix} S_{11} & S_{12} \\ S_{21} & S_{22} \end{bmatrix} \begin{bmatrix} a_{in} \\ b_{in} \end{bmatrix}$$

in which,

$$S_{11} = S_{22} = \frac{-i\Delta\omega + ig^2/(\Delta\omega - \delta)}{-i\Delta\omega + \gamma + ig^2/(\Delta\omega - \delta)}$$

and

$$S_{12} = S_{21} = \frac{-\gamma}{-i\Delta\omega + \gamma + ig^2/(\Delta\omega - \delta)}$$

Moreover,a_{out} and b_{out} are the annihilation operators of the output ports, and a_{in} and b_{in} are the annihilation operators of the input ports, while $\Delta\omega = \omega_{ph} - \omega_c$, $\delta = \omega_{atom} - \omega_c$, and γ is the rate of coupling from the cavity to each waveguide, and g is the atom-cavity coupling rate.

Based on these analytical solutions, without the presence of the atom, the cavity acts as a beam splitter [62] for any number of incident photons. For completeness, however, we have shown the numerical results of this case in Fig. 4. Assuming that the incident photon(s) are decoupled from the cavity with a decay rate of γ_{inc} and with a resonance frequency that is detuned by $\Delta\omega$ from the interacting cavity, the spectrum of the incident pulse is given by the Lorentzian form of $S(\omega) = \frac{2\gamma_{inc}}{\pi} \frac{1}{4(\omega - \Delta\omega - \omega_c)^2 + \gamma_{inc}^2}$. Using this fact and the above-mentioned scattering matrix, the total reflection in the first round of interaction is given by:

$$R = \frac{2\gamma(2\gamma + \gamma_{inc})}{(2\gamma + \gamma_{inc})^2 + 4\Delta\omega^2}$$

This analytical result is consistent with the reflection obtained numerically for two cases of $\gamma_{inc} = \gamma$ and $\gamma_{inc} = 0.04\gamma$, shown in Fig. 4a and 4b, respectively.

Furthermore, the scattering behavior for the more interesting case of the interaction of the out-coupled photons impinging on a cavity with a two-level atom inside is depicted in Fig. 6a. Here, we have assumed that the atom and incident photons are in resonance. For the case of a single photon, by assuming zero detuning between the cavity resonance frequency and the two-level atom and using the above-mentioned Lorentzian spectrum for the decoupled photon, the average number of reflected photons can be obtained by:

$$R = \frac{2\gamma_{inc}}{\pi} \int_{-\infty}^{\infty} \frac{d\omega}{4\Delta\omega^2 + \gamma_{inc}^2} \frac{\gamma^2}{\gamma^2 + (g^2/\Delta\omega - \Delta\omega)^2}$$

When $\gamma_{inc} = \gamma$, this results in $R = 0.5$ for $g = \gamma/2$. The numerically calculated reflection of a single photon as a function of atom-cavity coupling rate (Fig. 5a) is consistent with this analytical expression. The results of the interaction of multiple photons with a single atom located in a resonant cavity are also depicted in Fig. 5a. As this figure shows, by increasing the number of incident photons, the atom-cavity coupling rate must increase in order to reach a 50/50 splitting of the output photon ratios. This is consistent with our intuition, as more coupling is needed to redirect the path of a higher number of photons compared with the case of a single photon.

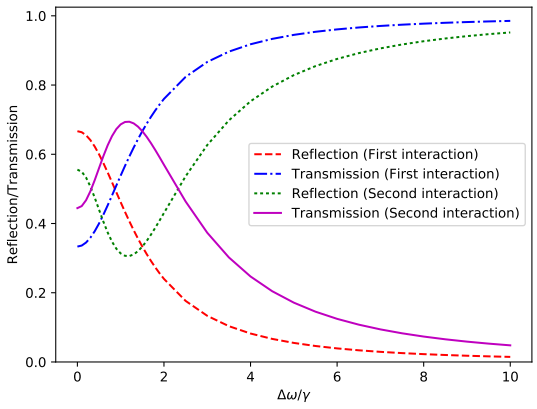

(a)

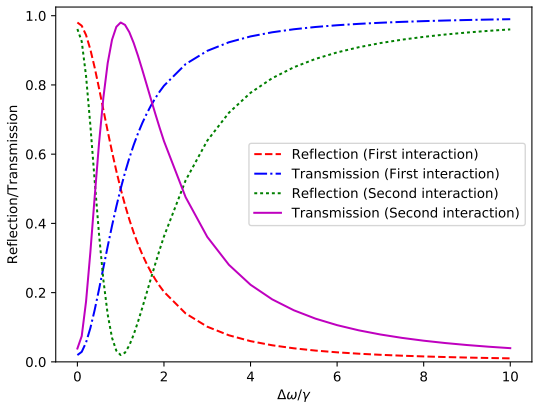

(b)

Figure 4: Reflection and transmission of the incident photons from a cavity as a function of their frequency shift from the cavity resonance frequency for the first two rounds of interactions. The incident photons are decoupled from the cavity with decay rates of (a) $\gamma_{inc} = \gamma$ and (b) $\gamma_{inc} = 0.04\gamma$.

In addition, the number of photons transmitted or reflected are calculated as a function of atom-cavity coupling rate in the second interaction. The results of these calculations are shown for the case of a single photon and two photons in Fig. 5b. There are deviations in both rounds of interactions between the results of these two cases. However, in the second round the scattering behavior for these two cases becomes closer as compared with the first round of interaction.

By assuming a smaller decay rate for the cavity from which incident photons are decoupled, we can also excite

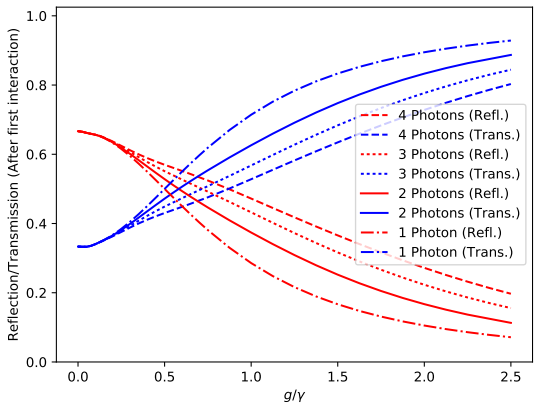

(a)

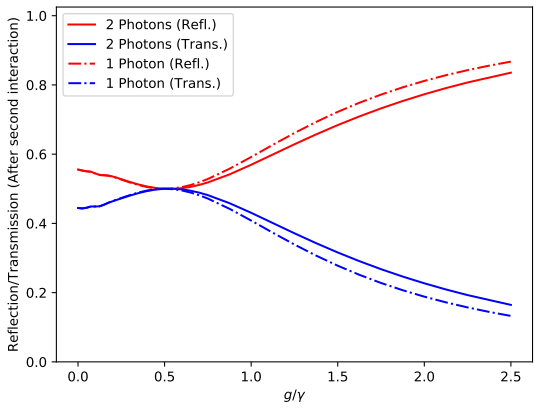

(b)

Figure 5: Reflection and transmission of the incident photons from a cavity as a function of atom-cavity coupling rate for the first two rounds of interactions. The incident photons are decoupled from a cavity with a decay rate of $\gamma_{inc} = \gamma$.

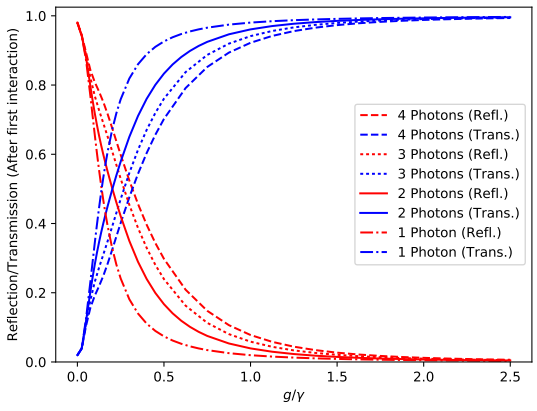

(a)

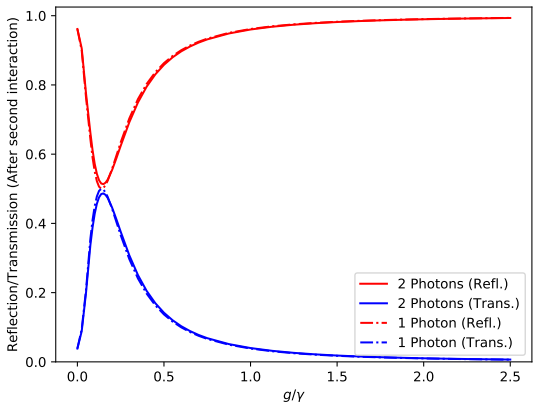

(b)

Figure 6: Reflection and transmission of the incident photons from a cavity as a function of atom-cavity coupling rate for the first two rounds of interactions. The incident photons are decoupled from the cavity with a decay rate of $\gamma_{inc} = 0.04\gamma$.

photons with smaller line-widths. The numerically obtained results for the reflection and transmission of multiple incident photons with a line-width of $\gamma_{inc} = 0.04\gamma$ in the first round are shown in Fig. 6a. The corresponding results in the second round for the case of a single photon or two incident photons are shown in Fig. 6b. These results again reveal the requirement of higher atom-cavity coupling rates to achieve a similar amount of transmission and reflection for the case of multiple photons as compared with a single photon.

For the case of $\gamma_{inc} = 0.04\gamma$, which closely models monochromatic photons, the second order correlation function for the decoupled photons in the top waveguide for the first round and in the bottom waveguide for the second round is shown in Figs. 7a and 7b, respectively. In the first round, $g_2(t)$ starts from 0.5 as dictated by the fixed photon number and increases due to stimulated emission to reach a maximum at a certain time. However, $g_2(t)$ then starts decreasing and asymptotically approaches 0.5 after a settling time proportional to $2\pi \,/\, g$, indicating that the photons are scattered by separate atom transitions. In the second round, there is similar initial and asymptotic behavior for $g_2(t)$. However, it starts with a descent and then moves toward a peak value.

In the systems considered in this work, we have assumed zero detuning between the two-level atom and the cavity. Moreover, any non-radiative loss mechanism is assumed to be zero. Nevertheless, the developed method can be used for analyzing multiple interactions of photons and the cavity under more general circumstances, including for instance an arbitrary detuning between the photons and the two-level atom or the cavity. Furthermore, any loss mechanism other than decoupling to the

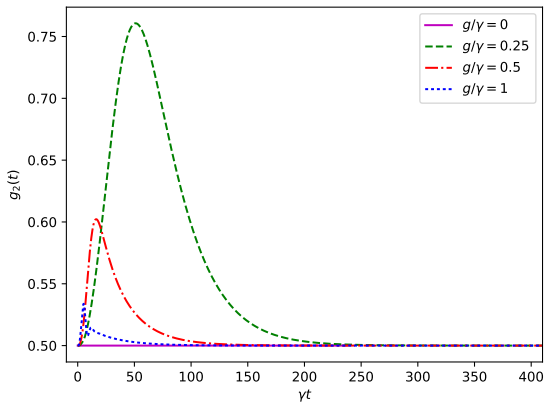

(a)

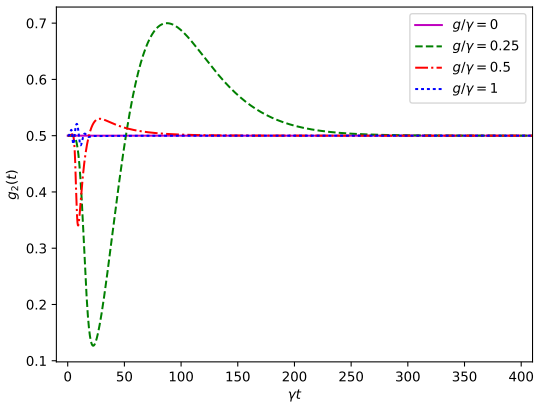

(b)

Figure 7: $g_2(t)$ for photons decoupled to the bottom and upper waveguides as a function of time in the (a) first and (b) second round, respectively.

waveguides, such as two-level atom non-radiative losses, can be included straightforwardly as extra collapse operators.

CONCLUSION

In this work, we have developed a method to obtain the evolution of a system under a bidirectional time-delayed feedback loop. For this purpose, we have expressed this evolution in terms of the time propagation of the actual system without feedback in addition to several systems identical to it which represent the system's past history. This method provides a numerically efficient solution when the time delays become comparable to the inverse of the decay rates. Under such conditions, directly tracking the state of the reservoirs representing the time-delayed feedbacks becomes numerically expensive. We have applied this method to investigate the scatterings of multiple photons incident on an atom-cavity system coupled to two waveguides that are connected at their ends. We have demonstrated how the number of incident photons as well as the delay between them affect their reflection and transmission from the atom-cavity system. The developed method can be used for studying a broad range of nonlinear dynamics in complex quantum networks.

ACKNOWLEDGMENTS

We wish to thank Prof. Mohammad Hafezi and Prof. Jacob Taylor for their helpful comments on this topic. This work was supported by the Physics Frontier Center at the Joint Quantum Institute, the National Science Foundation (grants PHY1415485 and ECCS1508897), the ARL Center for Distributed Quantum Information, and a grant from the Laboratory for Telecommunication Sciences. The majority of the calculations in this work were carried out in the high-performance computing resources (Deepthought2 cluster) provided by the University of Maryland.

[1] S. Boccaletti, C. Grebogi, Y.-C. Lai, H. Mancini, and D. Maza, Physics Reports **329**, 103 (2000).
[2] A. L. Fradkov and R. J. Evans, Annual Reviews in Control **29**, 33 (2005).
[3] "W. Michiels and S.-I. Niculescu, Stability and Stabilization of Time-Delay Systems (Society for Industrial and Applied Mathematics, Philadelphia, 2007).".
[4] K. Pyragas, Physics Letters A **170**, 421 (1992).
[5] A. Ahlborn and U. Parlitz, Phys. Rev. Lett. **93**, 264101 (2004).
[6] K. Pyragas, Philosophical Transactions of the Royal Society of London A: Mathematical, Physical and Engineering Sciences **364**, 2309 (2006), http://rsta.royalsocietypublishing.org/content/364/1846/2309.full.pdf.
[7] H. M. Wiseman and G. J. Milburn, Physical Review A **49**, 4110 (1994).
[8] S. Lloyd, Phys. Rev. A **62**, 022108 (2000).
[9] M. R. James, H. I. Nurdin, and I. R. Petersen, IEEE Transactions on Automatic Control **53**, 1787 (2008).
[10] H. Mabuchi, Phys. Rev. A **78**, 032323 (2008).
[11] J. E. Gough and S. Wildfeuer, Phys. Rev. A **80**, 042107 (2009).

[12] S. Iida, M. Yukawa, H. Yonezawa, N. Yamamoto, and A. Furusawa, IEEE Transactions on Automatic Control **57**, 2045 (2012).
[13] J. Kerckhoff and K. W. Lehnert, Phys. Rev. Lett. **109**, 153602 (2012).
[14] S. Shankar, M. Hatridge, Z. Leghtas, K. Sliwa, A. Narla, U. Vool, S. M. Girvin, L. Frunzio, M. Mirrahimi, and M. H. Devoret, Nature **504**, 419 (2013).
[15] J. Kerckhoff, D. S. Pavlichin, H. Chalabi, and H. Mabuchi, New Journal of Physics **13**, 055022 (2011).
[16] J. Kerckhoff, H. I. Nurdin, D. S. Pavlichin, and H. Mabuchi, Phys. Rev. Lett. **105**, 040502 (2010).
[17] K. Jacobs, X. Wang, and H. M. Wiseman, New Journal of Physics **16**, 073036 (2014).
[18] "C. Gardiner and P. Zoller, The Quantum World of Ultra-Cold Atoms and Light Book I: Foundations of Quantum Optics, 1st ed. (Imperial College Press, London, 2014)." ().
[19] "C. Gardiner and P. Zoller, The Quantum World of Ultra-Cold Atoms and Light Book II: The Physics of Quantum-Optical Devices, 1st ed. (Imperial College Press, London,2015)." ().
[20] R. Schoelkopf and S. Girvin, Nature **451**, 664 (2008).
[21] J. Gough and M. R. James, IEEE Transactions on Automatic Control **54**, 2530 (2009).
[22] A. Frisk Kockum, P. Delsing, and G. Johansson, Phys. Rev. A **90**, 013837 (2014).
[23] H. J. Kimble, Nature **453**, 1023 (2008).
[24] M. H. Devoret and R. J. Schoelkopf, Science **339**, 1169 (2013), http://science.sciencemag.org/content/339/6124/1169.full.pdf.
[25] R. Barends, J. Kelly, A. Megrant, A. Veitia, D. Sank, E. Jeffrey, T. C. White, J. Mutus, A. G. Fowler, B. Campbell, *et al.*, Nature **508**, 500 (2014).
[26] C. W. Gardiner, Phys. Rev. Lett. **70**, 2269 (1993).
[27] A. F. Van Loo, A. Fedorov, K. Lalumière, B. C. Sanders, A. Blais, and A. Wallraff, Science **342**, 1494 (2013).
[28] N. Roch, M. E. Schwartz, F. Motzoi, C. Macklin, R. Vijay, A. W. Eddins, A. N. Korotkov, K. B. Whaley, M. Sarovar, and I. Siddiqi, Phys. Rev. Lett. **112**, 170501 (2014).
[29] A. Goban, C.-L. Hung, S.-P. Yu, J. Hood, J. Muniz, J. Lee, M. Martin, A. McClung, K. Choi, D. E. Chang, *et al.*, Nature communications **5**, 3808 (2014).
[30] M. V. Gustafsson, T. Aref, A. F. Kockum, M. K. Ekström, G. Johansson, and P. Delsing, Science **346**, 207 (2014).
[31] "H. M. Wiseman and G. J. Milburn, Quantum Measurement and Control (Cambridge University Press, Cambridge,England, 2010).".
[32] A. Rivas, S. F. Huelga, and M. B. Plenio, Reports on Progress in Physics **77**, 094001 (2014).
[33] H.-P. Breuer, E.-M. Laine, J. Piilo, and B. Vacchini, Rev. Mod. Phys. **88**, 021002 (2016).
[34] W. T. Strunz, L. Diosi, and N. Gisin, Phys. Rev. Lett. **82**, 1801 (1999).
[35] A. L. Grimsmo, Phys. Rev. Lett. **115**, 060402 (2015).
[36] H. Pichler and P. Zoller, Phys. Rev. Lett. **116**, 093601 (2016).
[37] H. Pichler, S. Choi, P. Zoller, and M. D. Lukin, Proceedings of the National Academy of Sciences **114**, 11362 (2017), http://www.pnas.org/content/114/43/11362.full.pdf.
[38] M. Fannes, B. Nachtergaele, and R. F. Werner, Communications in mathematical physics **144**, 443 (1992).
[39] S. R. White, Phys. Rev. Lett. **69**, 2863 (1992).
[40] S. Ostlund and S. Rommer, Phys. Rev. Lett. **75**, 3537 (1995).
[41] G. Vidal, Phys. Rev. Lett. **93**, 040502 (2004).
[42] A. J. Daley, C. Kollath, U. Schollwöck, and G. Vidal, Journal of Statistical Mechanics: Theory and Experiment **2004**, P04005 (2004).
[43] U. Schollwock, Rev. Mod. Phys. **77**, 259 (2005).
[44] B. Peropadre, D. Zueco, D. Porras, and J. J. García-Ripoll, Phys. Rev. Lett. **111**, 243602 (2013).
[45] T. J. Osborne, J. Eisert, and F. Verstraete, Phys. Rev. Lett. **105**, 260401 (2010).
[46] F. Verstraete and J. I. Cirac, Phys. Rev. Lett. **104**, 190405 (2010).
[47] J. Haegeman, J. I. Cirac, T. J. Osborne, H. Verschelde, and F. Verstraete, Phys. Rev. Lett. **105**, 251601 (2010).
[48] C. Schön, K. Hammerer, M. M. Wolf, J. I. Cirac, and E. Solano, Phys. Rev. A **75**, 032311 (2007).
[49] C. Schon, E. Solano, F. Verstraete, J. I. Cirac, and M. M. Wolf, Phys. Rev. Lett. **95**, 110503 (2005).
[50] J.-T. Shen and S. Fan, Phys. Rev. A **76**, 062709 (2007).
[51] J.-T. Shen and S. Fan, Phys. Rev. Lett. **98**, 153003 (2007).
[52] J.-T. Shen, S. Fan, *et al.*, Physical Review A **79**, 023837 (2009).
[53] M. Laakso and M. Pletyukhov, Phys. Rev. Lett. **113**, 183601 (2014).
[54] Y.-L. L. Fang, F. Ciccarello, and H. U. Baranger, New Journal of Physics **20**, 043035 (2018).
[55] Y.-L. L. Fang and H. U. Baranger, Phys. Rev. A **91**, 053845 (2015).
[56] P.-O. Guimond, M. Pletyukhov, H. Pichler, and P. Zoller, Quantum Science and Technology **2**, 044012 (2017).
[57] A. Roulet and V. Scarani, New Journal of Physics **18**, 093035 (2016).
[58] A. Roulet, H. N. Le, and V. Scarani, Physical Review A **93**, 033838 (2016).
[59] I. Sollner, S. Mahmoodian, S. L. Hansen, L. Midolo, A. Javadi, G. Kirvsansk, T. Pregnolato, H. El-Ella, E. H. Lee, J. D. Song, *et al.*, Nature nanotechnology **10**, nnano (2015).
[60] R. Mitsch, C. Sayrin, B. Albrecht, P. Schneeweiss, and A. Rauschenbeutel, Nature communications **5**, 5713 (2014).
[61] E. Waks and J. Vuckovic, Phys. Rev. Lett. **96**, 153601 (2006).
[62] W.-X. Lai, H.-C. Li, X. Lin, and X. Chen, Phys. Rev. A **79**, 023832 (2009).
[63] R. Penrose, Combinatorial mathematics and its applications **1**, 221 (1971).
[64] C. J. Wood, J. D. Biamonte, and D. G. Cory, arXiv preprint arXiv:1111.6950 (2011).

APPENDIX:

ANALYSIS OF FEEDBACK LOOPS WITH SIMILAR TIME DELAYS

Following the approach introduced in [35], the evolution of the system under the feedback loop after several time delays can be expressed in terms of the evolution of the system and its replicas during a time delay, τ, followed by a generalized trace over the replicas. More precisely, in order to obtain the state of the actual system at time $t = k\tau + s$, we should obtain the evolution of the system and its k replicas from time 0 to s, as well as the evolution of the system and its $k-1$ replicas from time s to τ.

In order to get a sense of the evolution of the system and its replicas, we have considered in Fig. 8a (based on Penrose's tensor notation [35, 63, 64]) the evolution of the stacked systems after two time delays, $2\tau < t < 3\tau$. The analysis can easily be extended to the subsequent time delays. In this figure, U^{L_1} and U^{L_2} blocks represent the unitary superoperators acting on the system (horizontally) and the reservoir (vertically) that are connected to them. Specifically, U^{L_1} and U^{L_2} represent the evolution of the connected system and reservoir for an infinitesimal amount of time Δt corresponding to the coupling operators of L_1 and L_2, respectively.

As it can be seen from Fig. 8, the infinitesimal evolution of the stacked systems by Δt can itself be divided into four steps. Here, we represent the density matrix of the j^{th} system replica by ρ_{S_j} and the density matrix of the two connected reservoirs with ρ_{α_1} and ρ_{α_2}. Moreover, the annihilation operator for these two reservoirs are shown with b_n and c_n in which n represents the current time bin number. In addition, $L^{(j)}_{1,2}$ and $H^{(j)}_S$ represent the coupling operators and the Hamiltonian for j^{th} system, respectively.

In the first step, we will have:

$$\rho_{S_1}\otimes\rho_{\alpha_1} \to e^{-\frac{i\Delta t}{2}H_S^{(1)}+\sqrt{\Delta t}\left(L_2^{(1)}b_n^\dagger - L_2^{(1)\dagger}b_n\right)}\rho_{S_1}\otimes\rho_{\alpha_1} \times e^{\frac{i\Delta t}{2}H_S^{(1)}-\sqrt{\Delta t}\left(L_2^{(1)}b_n^\dagger - L_2^{(1)\dagger}b_n\right)}$$

Therefore, up to $(\Delta t)^{\frac{3}{2}}$, for $\rho_{\alpha_1} = |v\rangle_{\alpha_1}\langle v|_{\alpha_1} + O\left(\sqrt{\Delta t}\right)$ in which $|v\rangle_{\alpha_1}$ represents the vacuum state, we have:

$$\begin{aligned}
&\rho_{S_1}\otimes\rho_{\alpha_1} \to \rho_{S_1}\otimes\rho_{\alpha_1}\\
&+\sqrt{\Delta t}\left[L_2^{(1)}b_n^\dagger - L_2^{(1)\dagger}b_n, \rho_{S_1}\otimes\rho_{\alpha_1}\right]\\
&-\frac{\Delta t}{2}\left(i\left[H_S^{(1)},\rho_{S1}\right]+\left\{L_2^{(1)\dagger}L_2^{(1)},\rho_{S_1}\right\}\right)\otimes|v\rangle_{\alpha_1}\langle v|_{\alpha_1}\\
&+\Delta t L_2^{(1)}\rho_{S_1}L_2^{(1)\dagger}\otimes b_n^\dagger|v\rangle_{\alpha_1}\langle v|_{\alpha_1}b_n\\
&+\frac{\Delta t}{2}L_2^{(1)2}\rho_{S_1}\otimes b_n^{\dagger 2}|v\rangle_{\alpha_1}\langle v|_{\alpha_1}\\
&+\frac{\Delta t}{2}\rho_{S_1}L_2^{(1)\dagger 2}\otimes|v\rangle_{\alpha_1}\langle v|_{\alpha_1}b_n^2
\end{aligned}$$

In the second step, we will have:

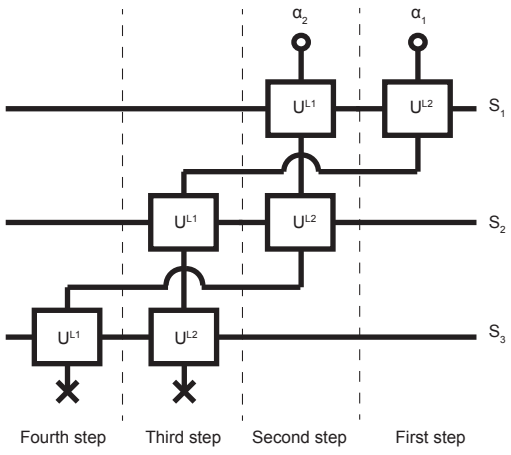

(a)

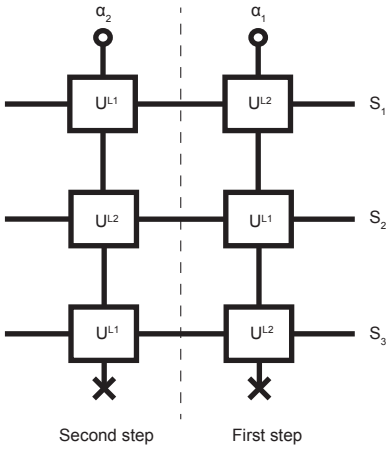

(b)

Figure 8: (a) An infinitesimal time evolution by Δt at time $2\tau < t = n\Delta t < 3\tau$ for the stacked systems (b) The same evolution by interchanging the blocks in every other row

$$\rho_{S_{1,2}}\otimes\rho_{\alpha_2}\to e^{-\frac{i\Delta t}{2}H_S^{(2)}+\sqrt{\Delta t}\left(L_2^{(2)}c_n^\dagger-L_2^{(2)\dagger}c_n\right)}\times e^{-\frac{i\Delta t}{2}H_S^{(1)}+\sqrt{\Delta t}\left(L_1^{(1)}c_n^\dagger-L_1^{(1)\dagger}c_n\right)}\rho_{S_{1,2}}\otimes\rho_{\alpha_2}\times e^{\frac{i\Delta t}{2}H_S^{(1)}-\sqrt{\Delta t}\left(L_1^{(1)}c_n^\dagger-L_1^{(1)\dagger}c_n\right)}e^{\frac{i\Delta t}{2}H_S^{(2)}-\sqrt{\Delta t}\left(L_2^{(2)}c_n^\dagger-L_2^{(2)\dagger}c_n\right)}$$

In which $\rho_{S_{1,2}}=\rho_{S_1}\otimes\rho_{S_2}$. We can define X and Y as:

$$X=-\frac{i\Delta t}{2}H_S^{(2)}+\sqrt{\Delta t}\left(L_2^{(2)}c_n^\dagger-L_2^{(2)\dagger}c_n\right)$$

$$Y=-\frac{i\Delta t}{2}H_S^{(1)}+\sqrt{\Delta t}\left(L_1^{(1)}c_n^\dagger-L_1^{(1)\dagger}c_n\right)$$

Since $\left[c_n,c_n^\dagger\right]=1$, it follows that:

$$[X,Y]=\Delta t\left(L_1^{(1)\dagger}L_2^{(2)}-L_1^{(1)}L_2^{(2)\dagger}\right)$$

Moreover, $[X,[X,Y]]=O\left((\Delta t)^{\frac{3}{2}}\right)$ and $[Y,[X,Y]]=O\left((\Delta t)^{\frac{3}{2}}\right)$. Therefore, up to $O\left((\Delta t)^{\frac{3}{2}}\right)$, from the Baker–Campbell–Hausdorff formula, $e^Xe^Y=e^{X+Y+\frac{1}{2}[X,Y]}$. Consequently, up to $O\left((\Delta t)^{\frac{3}{2}}\right)$, for $\rho_{\alpha_2}=|v\rangle_{\alpha_2}\langle v|_{\alpha_2}+O\left(\sqrt{\Delta t}\right)$, we have:

$$\begin{aligned}&\rho_{S_{1,2}}\otimes\rho_{\alpha_2}\to\rho_{S_{1,2}}\otimes\rho_{\alpha_2}\\&+\sqrt{\Delta t}\left[L_1^{(1)}c_n^\dagger+L_2^{(2)}c_n^\dagger-L_1^{(1)\dagger}c_n-L_2^{(2)\dagger}c_n,\rho_{S_{1,2}}\otimes\rho_{\alpha_2}\right]\\&-\frac{i\Delta t}{2}\left[H_S^{(1)}+H_S^{(2)},\rho_{S_{1,2}}\right]\otimes|v\rangle_{\alpha_2}\langle v|_{\alpha_2}\\&+\frac{\Delta t}{2}\left[L_1^{(1)\dagger}L_2^{(2)}-L_1^{(1)}L_2^{(2)\dagger},\rho_{S_{1,2}}\right]\otimes|v\rangle_{\alpha_2}\langle v|_{\alpha_2}\\&-\frac{\Delta t}{2}\left\{\left(L_1^{(1)}+L_2^{(2)}\right)^\dagger\left(L_1^{(1)}+L_2^{(2)}\right),\rho_{S_{1,2}}\right\}\otimes|v\rangle_{\alpha_2}\langle v|_{\alpha_2}\\&+\Delta t\left(L_1^{(1)}+L_2^{(2)}\right)\rho_{S_{1,2}}\left(L_1^{(1)}+L_2^{(2)}\right)^\dagger\otimes c_n^\dagger|v\rangle_{\alpha_2}\langle v|_{\alpha_2}c_n\\&+\frac{\Delta t}{2}\left(L_1^{(1)}+L_2^{(2)}\right)^2\rho_{S_{1,2}}\otimes c_n^{\dagger2}|v\rangle_{\alpha_2}\langle v|_{\alpha_2}\\&+\frac{\Delta t}{2}\rho_{S_{1,2}}\left(L_1^{(1)}+L_2^{(2)}\right)^{\dagger2}\otimes|v\rangle_{\alpha_2}\langle v|_{\alpha_2}c_n^2\end{aligned}$$

Similarly, in the third step:

$$\rho_{S_{2,3}}\otimes\rho_{\alpha_1}\to e^{\frac{-i\Delta t}{2}H_S^{(3)}+\sqrt{\Delta t}\left(L_2^{(3)}b_n^\dagger-L_2^{(3)\dagger}b_n\right)}\times e^{\frac{-i\Delta t}{2}H_S^{(2)}+\sqrt{\Delta t}\left(L_1^{(2)}b_n^\dagger-L_1^{(2)\dagger}b_n\right)}\rho_{S_{2,3}}\otimes\rho_{\alpha_1}\times e^{\frac{i\Delta t}{2}H_S^{(2)}-\sqrt{\Delta t}\left(L_1^{(2)}b_n^\dagger-L_1^{(2)\dagger}b_n\right)}e^{\frac{i\Delta t}{2}H_S^{(3)}-\sqrt{\Delta t}\left(L_2^{(3)}b_n^\dagger-L_2^{(3)\dagger}b_n\right)}$$

In which $\rho_{S_{2,3}}=\rho_{S_2}\otimes\rho_{S_3}$. Therefore, up to $(\Delta t)^{\frac{3}{2}}$, for $\rho_{\alpha_1}=|v\rangle_{\alpha_1}\langle v|_{\alpha_1}+O\left(\sqrt{\Delta t}\right)$, we have:

$$\begin{aligned}&\rho_{S_{2,3}}\otimes\rho_{\alpha_1}\to\rho_{S_{2,3}}\otimes\rho_{\alpha_1}\\&+\sqrt{\Delta t}\left[L_1^{(2)}b_n^\dagger+L_2^{(3)}b_n^\dagger-L_1^{(2)\dagger}b_n-L_2^{(3)\dagger}b_n,\rho_{S_{2,3}}\otimes\rho_{\alpha_1}\right]\\&-\frac{i\Delta t}{2}\left[H_S^{(2)}+H_S^{(3)},\rho_{S_{2,3}}\right]\otimes|v\rangle_{\alpha_1}\langle v|_{\alpha_1}\\&+\frac{\Delta t}{2}\left[L_1^{(2)\dagger}L_2^{(3)}-L_1^{(2)}L_2^{(3)\dagger},\rho_{S_{2,3}}\right]\otimes|v\rangle_{\alpha_1}\langle v|_{\alpha_1}\\&-\frac{\Delta t}{2}\left\{\left(L_1^{(2)}+L_2^{(3)}\right)^\dagger\left(L_1^{(2)}+L_2^{(3)}\right),\rho_{S_{2,3}}\right\}\otimes|v\rangle_{\alpha_1}\langle v|_{\alpha_1}\\&+\Delta t\left(L_1^{(2)}+L_2^{(3)}\right)\rho_{S_{2,3}}\left(L_1^{(2)}+L_2^{(3)}\right)^\dagger\otimes b_n^\dagger|v\rangle_{\alpha_1}\langle v|_{\alpha_1}b_n\\&+\frac{\Delta t}{2}\left(L_1^{(2)}+L_2^{(3)}\right)^2\rho_{S_{2,3}}\otimes b_n^{\dagger2}|v\rangle_{\alpha_1}\langle v|_{\alpha_1}\\&+\frac{\Delta t}{2}\rho_{S_{2,3}}\left(L_1^{(2)}+L_2^{(3)}\right)^{\dagger2}\otimes|v\rangle_{\alpha_1}\langle v|_{\alpha_1}b_n^2\end{aligned}$$

Finally, in the fourth step, we have:

$$\rho_{S_3}\otimes\rho_{\alpha_2}\to e^{-\frac{i\Delta t}{2}H_S^{(3)}+\sqrt{\Delta t}\left(L_1^{(3)}c_n^\dagger-L_1^{(3)\dagger}c_n\right)}\rho_{S_3}\otimes\rho_{\alpha_2}\times e^{\frac{i\Delta t}{2}H_S^{(3)}-\sqrt{\Delta t}\left(L_1^{(3)}c_n^\dagger-L_1^{(3)\dagger}c_n\right)}$$

Therefore, up to $(\Delta t)^{\frac{3}{2}}$, for $\rho_{\alpha_2}=|v\rangle_{\alpha_2}\langle v|_{\alpha_2}+O\left(\sqrt{\Delta t}\right)$, we have:

$$\begin{aligned}&\rho_{S_3}\otimes\rho_{\alpha_2}\to\rho_{S_3}\otimes\rho_{\alpha_2}\\&+\sqrt{\Delta t}\left[L_1^{(3)}c_n^\dagger-L_1^{(3)\dagger}c_n,\rho_{S_3}\otimes\rho_{\alpha_2}\right]\\&-\frac{\Delta t}{2}\left(i\left[H_S^{(3)},\rho_{S_3}\right]+\left\{L_1^{(3)\dagger}L_1^{(3)},\rho_{S_3}\right\}\right)\otimes|v\rangle_{\alpha_2}\langle v|_{\alpha_2}\\&+\Delta tL_1^{(3)}\rho_{S_3}L_1^{(3)\dagger}\otimes c_n^\dagger|v\rangle_{\alpha_2}\langle v|_{\alpha_2}c_n\\&+\frac{\Delta t}{2}L_1^{(3)2}\rho_{S_3}\otimes c_n^{\dagger2}|v\rangle_{\alpha_2}\langle v|_{\alpha_2}\\&+\frac{\Delta t}{2}\rho_{S_3}L_1^{(3)\dagger^2}\otimes|v\rangle_{\alpha_2}\langle v|_{\alpha_2}c_n^2\end{aligned}$$

After the above four steps and by starting from vacuum states for ρ_{α_1} and ρ_{α_2}, followed by tracing over them and after simplification we obtain:

$$\begin{aligned}&\rho=\rho_{S_1}\otimes\rho_{S_2}\otimes\rho_{S_3}\to\rho-i\Delta t\left[H_{eff},\rho\right]\\&+\Delta t\left(L_1^{(1)}+L_2^{(2)}+L_1^{(3)}\right)\rho\left(L_1^{(1)}+L_2^{(2)}+L_1^{(3)}\right)^\dagger\\&-\frac{\Delta t}{2}\left\{\left(L_1^{(1)}+L_2^{(2)}+L_1^{(3)}\right)^\dagger\left(L_1^{(1)}+L_2^{(2)}+L_1^{(3)}\right),\rho\right\}\\&+\Delta t\left(L_2^{(1)}+L_1^{(2)}+L_2^{(3)}\right)\rho\left(L_2^{(1)}+L_1^{(2)}+L_2^{(3)}\right)^\dagger\\&-\frac{\Delta t}{2}\left\{\left(L_2^{(1)}+L_1^{(2)}+L_2^{(3)}\right)^\dagger\left(L_2^{(1)}+L_1^{(2)}+L_2^{(3)}\right),\rho\right\}\end{aligned}$$

In which:

$$
\begin{aligned}
H_{eff} &= H_S^{(1)} + H_S^{(2)} + H_S^{(3)} \\
&+ \frac{i}{2}\left(L_1^{(1)\dagger}L_2^{(2)} + L_1^{(2)\dagger}L_2^{(3)} - L_1^{(1)}L_2^{(2)\dagger} - L_1^{(2)}L_2^{(3)\dagger}\right) \\
&+ \frac{i}{2}\left(L_1^{(1)\dagger}L_1^{(3)} + L_2^{(2)\dagger}L_1^{(3)} - L_1^{(1)}L_1^{(3)\dagger} - L_2^{(2)}L_1^{(3)\dagger}\right) \\
&+ \frac{i}{2}\left(L_2^{(1)\dagger}L_1^{(2)} + L_2^{(1)\dagger}L_2^{(3)} - L_2^{(1)}L_1^{(2)\dagger} - L_2^{(1)}L_2^{(3)\dagger}\right)
\end{aligned}
$$

Noting the fact that the series blocks can be interchanged with each other, we could also obtain the same result based on the schematic depicted in Fig. 8b. Based on this schematic, the time evolution for infinitesimal time Δt at time t can be explained in terms of two consecutive steps. In the first step, we would have:

$$
\begin{aligned}
&\rho\otimes\rho_{\alpha_1} \to e^{\frac{-i\Delta t}{2}H_S^{(3)}+\sqrt{\Delta t}\left(L_2^{(3)}b_n^\dagger - L_2^{(3)\dagger}b_n\right)} \\
&\times e^{\frac{-i\Delta t}{2}H_S^{(2)}+\sqrt{\Delta t}\left(L_1^{(2)}b_n^\dagger - L_1^{(2)\dagger}b_n\right)} e^{\frac{-i\Delta t}{2}H_S^{(1)}+\sqrt{\Delta t}\left(L_2^{(1)}b_n^\dagger - L_2^{(1)\dagger}b_n\right)} \\
&\times \rho\otimes\rho_{\alpha_1} e^{\frac{i\Delta t}{2}H_S^{(1)}-\sqrt{\Delta t}\left(L_2^{(1)}b_n^\dagger - L_2^{(1)\dagger}b_n\right)} \\
&\times e^{\frac{i\Delta t}{2}H_S^{(2)}-\sqrt{\Delta t}\left(L_1^{(2)}b_n^\dagger - L_1^{(2)\dagger}b_n\right)} e^{\frac{i\Delta t}{2}H_S^{(3)}-\sqrt{\Delta t}\left(L_2^{(3)}b_n^\dagger - L_2^{(3)\dagger}b_n\right)}
\end{aligned}
$$

In the next step, we would have:

$$
\begin{aligned}
&\rho\otimes\rho_{\alpha_2} \to e^{\frac{-i\Delta t}{2}H_S^{(3)}+\sqrt{\Delta t}\left(L_1^{(3)}c_n^\dagger - L_1^{(3)\dagger}c_n\right)} \\
&\times e^{\frac{-i\Delta t}{2}H_S^{(2)}+\sqrt{\Delta t}\left(L_2^{(2)}c_n^\dagger - L_2^{(2)\dagger}c_n\right)} e^{\frac{-i\Delta t}{2}H_S^{(1)}+\sqrt{\Delta t}\left(L_1^{(1)}c_n^\dagger - L_1^{(1)\dagger}c_n\right)} \\
&\times \rho\otimes\rho_{\alpha_2} e^{\frac{i\Delta t}{2}H_S^{(1)}-\sqrt{\Delta t}\left(L_1^{(1)}c_n^\dagger - L_1^{(1)\dagger}c_n\right)} \\
&\times e^{\frac{i\Delta t}{2}H_S^{(2)}-\sqrt{\Delta t}\left(L_2^{(2)}c_n^\dagger - L_2^{(2)\dagger}c_n\right)} e^{\frac{i\Delta t}{2}H_S^{(3)}-\sqrt{\Delta t}\left(L_1^{(3)}c_n^\dagger - L_1^{(3)\dagger}c_n\right)}
\end{aligned}
$$

Using the Baker–Campbell–Hausdorff formula for each of these steps as it was used above, we obtain for the first step:

$$
\begin{aligned}
&\rho\otimes\rho_{\alpha_1} \to e^{\frac{-i\Delta t}{2}H_{eff,1st}+\sqrt{\Delta t}\left(\left(L_2^{(1)}+L_1^{(2)}+L_2^{(3)}\right)b_n^\dagger - h.c.\right)} \\
&\times \rho\otimes\rho_{\alpha_1} e^{\frac{i\Delta t}{2}H_{eff,1st}-\sqrt{\Delta t}\left(\left(L_2^{(1)}+L_1^{(2)}+L_2^{(3)}\right)b_n^\dagger - h.c.\right)}
\end{aligned}
$$

in which, $H_{eff,1st} = H_S^{(1)} + H_S^{(2)} + H_S^{(3)} + i\left(L_2^{(1)\dagger}L_1^{(2)} + L_1^{(2)\dagger}L_2^{(3)} + L_2^{(1)\dagger}L_2^{(3)} - h.c.\right)$.

Similarly, for the next step, we would obtain:

$$
\begin{aligned}
&\rho\otimes\rho_{\alpha_2} \to e^{\frac{-i\Delta t}{2}H_{eff,2nd}+\sqrt{\Delta t}\left(\left(L_1^{(1)}+L_2^{(2)}+L_1^{(3)}\right)c_n^\dagger - h.c.\right)} \\
&\times \rho\otimes\rho_{\alpha_2} e^{\frac{i\Delta t}{2}H_{eff,2nd}-\sqrt{\Delta t}\left(\left(L_1^{(1)}+L_2^{(2)}+L_1^{(3)}\right)c_n^\dagger - h.c.\right)}
\end{aligned}
$$

in which, $H_{eff,2nd} = H_S^{(1)} + H_S^{(2)} + H_S^{(3)} + i\left(L_1^{(1)\dagger}L_2^{(2)} + L_1^{(1)\dagger}L_1^{(3)} + L_2^{(2)\dagger}L_1^{(3)} - h.c.\right)$.

Starting from vacuum states for ρ_{α_1} and ρ_{α_2}, followed by tracing over them, we obtain a similar result as the one obtained above using four steps.

The above results can easily be generalized to the case when we are considering more than three time delays. If we show the delay as τ with $t = k\tau + s$, such that $0 < s < \tau$, then we need to consider $k+1$ identical systems. Using the above approach, we find that the time evolution for infinitesimal time Δt for $\rho = \rho_{S_1}\otimes\cdots\otimes\rho_{S_{k+1}}$ can be represented as the consecutive actions of the following two steps. In the first step, we would have:

$$
\begin{aligned}
&\rho\otimes\rho_{\alpha_1} \to \\
&e^{\frac{-i\Delta t}{2}H_S^{(k+1)}+\sqrt{\Delta t}\left(L_{(k+1)\bmod 2+1}^{(k+1)}b_n^\dagger - L_{(k+1)\bmod 2+1}^{(k+1)\dagger}b_n\right)} \\
&\times\cdots e^{\frac{-i\Delta t}{2}H_S^{(1)}+\sqrt{\Delta t}\left(L_2^{(1)}b_n^\dagger - L_2^{(1)\dagger}b_n\right)}\rho\otimes\rho_{\alpha_1} \\
&\times e^{\frac{i\Delta t}{2}H_S^{(1)}-\sqrt{\Delta t}\left(L_2^{(1)}b_n^\dagger - L_2^{(1)\dagger}b_n\right)}\cdots \\
&\times e^{\frac{i\Delta t}{2}H_S^{(k+1)}-\sqrt{\Delta t}\left(L_{(k+1)\bmod 2+1}^{(k+1)}b_n^\dagger - L_{(k+1)\bmod 2+1}^{(k+1)\dagger}b_n\right)} \\
&= e^{-\frac{i\Delta t}{2}H_{eff,1st}+\sqrt{\Delta t}\left(b_n^\dagger\sum_{q=0}^{k}L_{(q+1)\bmod 2+1}^{(q+1)} - h.c.\right)}\rho\otimes\rho_{\alpha_1} \\
&\times e^{\frac{i\Delta t}{2}H_{eff,1st}-\sqrt{\Delta t}\left(b_n^\dagger\sum_{q=0}^{k}L_{(q+1)\bmod 2+1}^{(q+1)} - h.c.\right)}
\end{aligned}
$$

in which, $H_{eff,1st} = \sum_{q=0}^{k}H_S^{(q+1)} + i\sum_{q=0}^{k-1}\sum_{j=q+1}^{k}\left(L_{(q+1)\bmod 2+1}^{(q+1)\dagger}L_{(j+1)\bmod 2+1}^{(j+1)} - h.c.\right)$.

And in the second step, we would have:

$$
\begin{aligned}
&\rho\otimes\rho_{\alpha_2} \to e^{\frac{-i\Delta t}{2}H_S^{(k+1)}+\sqrt{\Delta t}\left(L_{k\bmod 2+1}^{(k+1)}c_n^\dagger - L_{k\bmod 2+1}^{(k+1)\dagger}c_n\right)} \\
&\times\cdots e^{\frac{-i\Delta t}{2}H_S^{(1)}+\sqrt{\Delta t}\left(L_1^{(1)}c_n^\dagger - L_1^{(1)\dagger}c_n\right)}\rho\otimes\rho_{\alpha_2} \\
&\times e^{\frac{i\Delta t}{2}H_S^{(1)}-\sqrt{\Delta t}\left(L_1^{(1)}c_n^\dagger - L_1^{(1)\dagger}c_n\right)}\cdots \\
&\times e^{\frac{i\Delta t}{2}H_S^{(k+1)}-\sqrt{\Delta t}\left(L_{k\bmod 2+1}^{(k+1)}c_n^\dagger - L_{k\bmod 2+1}^{(k+1)\dagger}c_n\right)} \\
&= e^{-\frac{i\Delta t}{2}H_{eff,2nd}+\sqrt{\Delta t}\left(c_n^\dagger\sum_{q=0}^{k}L_{q\bmod 2+1}^{(q+1)} - h.c.\right)}\rho\otimes\rho_{\alpha_2} \\
&\times e^{\frac{i\Delta t}{2}H_{eff,2nd}-\sqrt{\Delta t}\left(c_n^\dagger\sum_{q=0}^{k}L_{q\bmod 2+1}^{(q+1)} - h.c.\right)}
\end{aligned}
$$

in which, $H_{eff,2nd} = \sum_{q=0}^{k}H_S^{(q+1)} + i\sum_{q=0}^{k-1}\sum_{j=q+1}^{k}\left(L_{q\bmod 2+1}^{(q+1)\dagger}L_{j\bmod 2+1}^{(j+1)} - h.c.\right)$.

Combining them we realize that the stacked systems' evolution can be described by the following Lindblad operators and effective Hamiltonian for time 0 to s.

$$H_{eff} = \sum_{q=0}^{k} H_S^{(q+1)} + \frac{i}{2}\sum_{q=0}^{k-1}\sum_{j=q+1}^{k} L_{q \bmod 2+1}^{(q+1)\dagger} L_{j \bmod 2+1}^{(j+1)} + \frac{i}{2}\sum_{q=0}^{k-1}\sum_{j=q+1}^{k} L_{(q+1) \bmod 2+1}^{(q+1)\dagger} L_{(j+1) \bmod 2+1}^{(j+1)} + h.c.$$

$$L_F = \sum_{q=0}^{k} L_{(q+1) \bmod 2+1}^{(q+1)}$$

$$L_B = \sum_{q=0}^{k} L_{q \bmod 2+1}^{(q+1)}$$

The evolution from time s to τ can be described by the above operators, however, by changing k with $k-1$ for $k>1$ and by unitary operation for $k=1$.

ANALYSIS OF FEEDBACK LOOPS WITH DIFFERENT TIME DELAYS

We can generalize the above approach to feedback loops with different time delays. For this purpose, we assume that the two delays can be represented as an integer multiplied by their common factor, such that $\tau_1 = n_1\tau$ and $\tau_2 = n_2\tau$. We are interested to obtain the evolution of the system up to $t = k\tau + s$. We first obtain the evolution from time 0 to s for the stacked systems. The evolution from s to τ will be obtained by replacing k with $k-1$.

Let us consider the evolution from time 0 to time s. For this, we should consider the stack of $k+1$ system replicas. In this more generalized scheme, the output field of the first $L_2^{(q+1)}$ block is connected to the input of the $L_1^{(q+n_2+1)}$ block and its output correspondingly is connected to the input of $L_2^{(q+n_1+n_2+1)}$, and this trend continues. Similarly, $L_1^{(q+1)}$, $L_2^{(q+n_1+1)}$, and $L_1^{(q+n_2+n_1+1)}$ blocks and so on are connected. Therefore, there exists the following effective Hamiltonian and Lindblad operators:

$$H_{eff} = \sum_{q=0}^{k} H_S^{(q+1)} + V_{int}$$

$$L_{F,l} = \sum_{j=0}\left(L_2^{(l+jn_t+1)} + L_1^{(l+jn_t+n_2+1)}\right) \quad 0 \le l < n_1$$

$$L_{B,p} = \sum_{j=0}\left(L_1^{(p+jn_t+1)} + L_2^{(p+jn_t+n_1+1)}\right) \quad 0 \le p < n_2$$

In the above equations, $n_t = n_1 + n_2$ and V_{int} represents the interaction terms between system replicas caused by L blocks connections, which is a summation of the terms each with the form of $\frac{i}{2}\left(L_{1,2}^{q\dagger} L_{2,1}^{j} - h.c.\right)$.

Moreover, a note should be added that in the above summations, the upper limit is determined by the fact that we only consider terms $L_{1,2}^{(l)}$ for $l \le k+1$.

For instance, let us consider the case that $\tau_2 = m\tau_1 = m\tau$. The L operators are as the followings:

$$L_F = \sum_{j=0}\left(L_2^{((m+1)j+1)} + L_1^{((m+1)j+m+1)}\right)$$

$$L_{B,p} = \sum_{j=0}\left(L_1^{((m+1)j+p+1)} + L_2^{((m+1)j+p+2)}\right) \quad 0 \le p < m$$

The interaction term in this case is given by:

$$\begin{aligned} V_{int} = {} & \frac{i}{2}\sum_{j=0}\sum_{l=j+1} L_2^{((m+1)j+1)\dagger}\left(L_2^{((m+1)l+1)} + L_1^{((m+1)l)}\right) \\ & + \frac{i}{2}\sum_{j=0}\sum_{l=j+1} L_1^{((m+1)(j+1))\dagger}\left(L_2^{((m+1)l+1)} + L_1^{((m+1)(l+1))}\right) \\ & + \frac{i}{2}\sum_{p=0}^{m-1}\sum_{j=0}\sum_{l=j+1} L_1^{((m+1)j+p+1)\dagger} L_1^{((m+1)l+p+1)} \\ & + \frac{i}{2}\sum_{p=0}^{m-1}\sum_{j=0}\sum_{l=j+1} L_1^{((m+1)j+p+1)\dagger} L_2^{((m+1)(l-1)+p+2)} \\ & + \frac{i}{2}\sum_{p=0}^{m-1}\sum_{j=0}\sum_{l=j+1} L_2^{((m+1)j+p+2)\dagger} L_1^{((m+1)l+p+1)} \\ & + \frac{i}{2}\sum_{p=0}^{m-1}\sum_{j=0}\sum_{l=j+1} L_2^{((m+1)j+p+2)\dagger} L_2^{((m+1)l+p+2)} + h.c. \end{aligned}$$

For the case of $m=2$, these can be simplified even further to:

$$\begin{aligned} V_{int} = {} & \frac{i}{2}\sum_{J=1}\sum_{l=0} L_1^{(J)\dagger}\left(L_1^{(J+3l+3)} + L_2^{(J+3l+1)}\right) \\ & + \frac{i}{2}\sum_{J=1}\sum_{l=0} L_2^{(J)\dagger}\left(L_1^{(J+3l+2)} + L_2^{(J+3l+3)}\right) + h.c. \end{aligned}$$

and:

$$L_F = \sum_{j=0}\left(L_2^{(3j+1)} + L_1^{(3j+3)}\right)$$

$$L_{B,0} = \sum_{j=0}\left(L_1^{(3j+1)} + L_2^{(3j+2)}\right)$$

$$L_{B,1} = \sum_{j=0}\left(L_1^{(3j+2)} + L_2^{(3j+3)}\right)$$

For the case of $\tau_1 = 2\tau$ and $\tau_2 = 3\tau$, the L operators are as follows:

$$L_{F,l} = \sum_{j=0} \left(L_2^{(l+5j+1)} + L_1^{(l+5j+4)} \right) \quad 0 \leq l < 2$$
$$L_{B,p} = \sum_{j=0} \left(L_1^{(p+5j+1)} + L_2^{(p+5j+3)} \right) \quad 0 \leq p < 3$$

The interaction term in this case can be simplified to:

$$V_{int} = \frac{i}{2} \sum_{J=1} \sum_{l=0} L_1^{(J)\dagger} \left(L_1^{(J+5l+5)} + L_2^{(J+5l+2)} \right) + \frac{i}{2} \sum_{J=1} \sum_{l=0} L_2^{(J)\dagger} \left(L_1^{(J+5l+3)} + L_2^{(J+5l+5)} \right) + h.c.$$

Similar results can be obtained for the general case of $\tau_1 = n_1\tau$ and $\tau_2 = n_2\tau$ for integer values of n_1 and n_2.

In the simple case of a cavity with a single photon inside, we can investigate the effect of a bidirectional time-delayed feedback loop based on the above presented method. We have considered cavity photon number variation for two overall phase shifts of $\phi = 0$ and $\phi = \pi$, in Figs. 9a and 9b, respectively. For each phase, assuming $\gamma\tau = 1$, four cases of $\tau_1 = \tau$, $\tau_2 = \infty$ and $\tau_2 = \tau_1 = \tau$ and $\tau_2 = 2\tau_1 = 2\tau$, as well as $\tau_1 = 2\tau$, $\tau_2 = 3\tau$ are shown for comparison. In the special case of $\tau_1 = \tau$, $\tau_2 = \infty$ [35], the constructive and destructive interference happening for two phases of $\phi = 0$ and $\phi = \pi$ will lead to a zero or a constant occupation number in the steady state, respectively. However, in the other three cases, these figures show that there is an oscillatory behavior for the occupation number as a function of time.

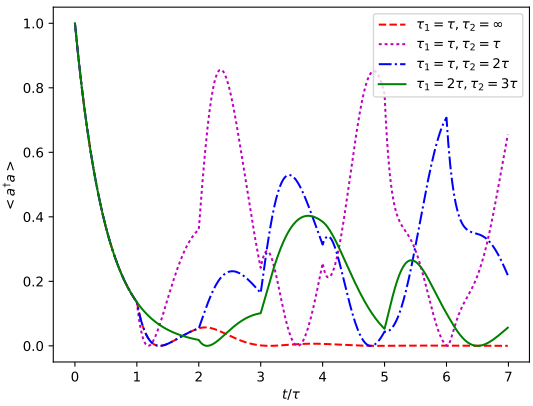

(a)

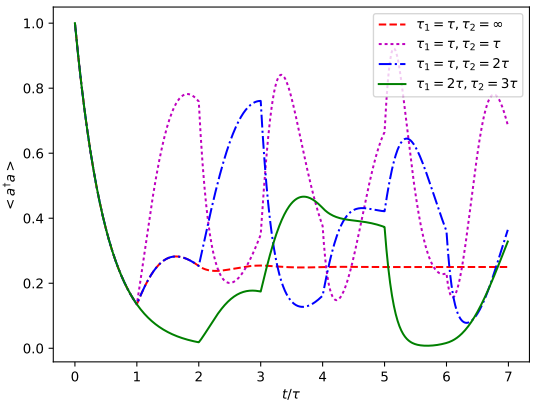

(b)

Figure 9: The variation of cavity photon number as a function of time under different bidirectional time-delayed feedback loops for two overall phase shifts of (a) $\phi = 0$ and (b) $\phi = \pi$ between the ports.